


Semiclassical theory of laser-assisted radiative recombination

I. I. Fabrikant  and H. B. Ambalampitiya 

Department of Physics and Astronomy, University of Nebraska–Lincoln, Lincoln, Nebraska 68588-0299, USA



(Received 28 February 2020; revised manuscript received 7 April 2020; accepted 9 April 2020; published 4 May 2020)

We study the process of laser-assisted radiative recombination of an electron with a proton by using a semiclassical approach involving calculation of classical trajectories in combined laser and Coulomb fields. Due to chaotic scattering in the combined fields, the radiation probability as a function of the impact parameter and the constant phase of the laser field exhibits chaotic behavior and fractal structures. We obtain a strong enhancement of the recombination cross section as compared to the laser-free case due to the Coulomb focusing effect. For sufficiently low incident electron velocities the cross section becomes infinite, and we limit it by assuming a finite laser pulse duration. With the pulse duration $t_p = 5$ ps we obtain the gain factor for capture into the ground state of the hydrogen atom of about 220 for infrared fields in the intensity range 10^9 – 10^{12} W/cm². The gain factor grows with t_p but slower than linearly.

DOI: [10.1103/PhysRevA.101.053401](https://doi.org/10.1103/PhysRevA.101.053401)

I. INTRODUCTION

Spontaneous radiative recombination (RR)

$$e^- + A^{+(n)} \rightarrow A^{+(n-1)} + h\nu$$

is an important process in plasmas [1,2] and in electron cooling in ion beams [3,4]. In 1983 Neumann *et al.* [5] proposed to use it for formation of antihydrogen atoms through a similar reaction involving positron capture by antiproton. Since the rate of spontaneous RR is very small, they proposed to increase it by using a *stimulated* RR of the type

$$e^- + A^{+(n)} + h\nu \rightarrow A^{+(n-1)} + 2h\nu.$$

The ratio of the stimulated recombination rate to the spontaneous recombination rate is called the gain factor. In their storage ring experiments, Schramm *et al.* [6] were able to obtain the gain factor up to 22 for capture into the $n = 2$ state of the hydrogen atom. In similar experiments, Mitchell's group [7,8] found that the value of the gain factor reached up to a few thousand for capture into Rydberg states with principal quantum numbers of $n = 11, 12$, and 13.

The rate of the stimulated RR is proportional to the laser intensity. However, in practice the intensity is limited by the competing process of photoionization. Indeed, according to the Einstein theory of stimulated emission, the ratio of the stimulated emission rate W^{SiRR} to the photoionization rate W^{PI} is [5]

$$\frac{W^{\text{SiRR}}}{W^{\text{PI}}} = \frac{\pi^2 \hbar^2 j}{m E_e \Delta\nu},$$

where m is the electron mass, E_e is the electron energy, j is the electron current density, and $\Delta\nu$ is the spectral width of the radiation field. This ratio is very small for realistic parameters j and $\Delta\nu$. However, at low intensities, when both rates are small, the capture into an excited state is accompanied by another competing process, spontaneous emission into a lower state. If we require that this process happens faster than

photoionization, for intensity we obtain

$$I < \frac{h\nu}{\sigma^{\text{PI}} \tau},$$

where σ^{PI} is the photoionization cross section, and τ is the lifetime with respect to the spontaneous emission. For the $2p$ state of hydrogen, $\tau = 1.6$ ns. Using this lifetime, Schramm *et al.* [6] estimated that under the conditions of their storage ring experiment the restriction for intensity is $I < 20$ MW/cm². With this restriction they were able to achieve the gain factor up to 22. Mitchell's group [7,8] was able to prevent reionization by limiting the duration of the laser pulse. However, attempts to use laser-stimulated RR for antihydrogen production in the $n = 11$ state by the ATHENA collaboration [9] demonstrated no evidence for this process, apparently because the $e^+ + \bar{p}$ RR to the $n = 11$ state of $\bar{\text{H}}$ has a much lower cross section than that for the three-body recombination, which is the dominant process in the ATHENA experiment [10].

In the present paper we discuss an alternative method to increase the RR rate—the *laser-assisted* recombination. In contrast to the stimulated recombination, the laser-assisted recombination is a nonresonant process, since the frequency of the laser field is not equal to the emitted photon frequency. The advantage of the laser-assisted, rather than stimulated, emission is that the reionization process in the latter could be relatively weak. Indeed, for a low-frequency field one-photon ionization is not possible. The laser intensity should still be limited due to the possibility of tunneling ionization in strong fields. However, the restriction on intensity is not as strong as for the stimulated emission.

The laser-assisted RR is the final step of the higher-order harmonic generation process (HHG) [11–13] when an electron is captured by an ion by emitting a high-frequency photon in an infrared field. This was studied experimentally in this context in Refs. [14,15], whereby continuum electrons were created by photoionization of Ca and Ba atoms with a

subsequent observation of radiative recombination in a half-cycle electric field pulse [14] or a microwave field [15,16]. A strong enhancement of RR into Rydberg states by a half-cycle laser pulse was studied theoretically in [17,18]. More recent theoretical papers on laser-assisted RR [19–27] were focused on relatively high-energy electrons (hundreds of eV) capable of producing x rays. The Coulomb effects were either neglected or treated perturbatively, which can be justified for strong fields and high-energy electrons. However, the cross sections for RR in these cases are rather small. In contrast, in the present paper we concentrate on low-energy electrons with velocities of about or below 0.2 a.u. (energy below 0.54 eV) when the Coulomb effects are important and the cross sections become large.

A complete quantum treatment of electron motion in combined laser and Coulomb fields, although possible by numerical solution of the time-dependent Schrödinger equation [28–32], presents big challenges and lacks physical transparency. Fortunately, sometimes processes involving electron motion in a superposition of laser and Coulomb fields can be treated classically. A typical example is electron bremsstrahlung, or a continuum-continuum radiative transition. At low electron velocities the motion in the Coulomb field is quasiclassical [33], specifically, for the motion in the Coulomb field “the condition for quasiclassical motion... can be written in the form $\alpha/\hbar v \gg 1$ ” [33] (α is the Coulomb constant). In particular, comparison of classical and quantum cross sections for bremsstrahlung in the Coulomb field shows good agreement [34]. This conclusion was used [34] to calculate laser-assisted bremsstrahlung. Two important features have been found. First, since classical scattering in combined fields is chaotic [35–37], the emission probability is a random function of the impact parameter and the constant phase of the laser field. The latter feature was used [38] to explain the plateau behavior of the above-threshold ionization. Second, due to the effect of Coulomb focusing [39], a very wide range of impact parameters contributes to the emission process, resulting in a cross section which is much larger than that for the laser-free bremsstrahlung. The Coulomb focusing has been studied previously in the process of strong-field ionization [39–45] and HHG [46]. However, in these two processes the range of impact parameters is strongly limited, since the processes start with a bound electron. In contrast, the processes of free-free and free-bound transitions start with an unbound electron; therefore the range of impact parameters contributing to the processes is much wider, and the cross section enhancement is much more substantial.

In contrast to bremsstrahlung, the RR process cannot be treated completely classically, since the electron is captured into a bound quantum state. However, even before the development of quantum mechanics, Kramers [47] used the Bohr theory and correspondence principle to derive semiclassical expressions for cross sections for photoionization and RR. The Kramers formula works surprisingly well even for the ground state. Specifically, the Kramers photoionization cross section from the $1s$ state of the hydrogen atom exceeds the exact quantum-mechanical result [48] at the photoionization threshold by only about 25%, and agreement is improving with the growth of the photon energy. Berson [49] used the same approach to derive a semiclassical formula for

multiphoton ionization. Comparison with quantum results shows that Berson’s formula works very well if $n \geq N_m$, where N_m is the minimum number of photons required for ionization.

In the present paper we use the Kramers approach to treat laser-assisted RR. Similar to the laser-assisted bremsstrahlung case [34], the cross section is strongly increased as compared to the laser-free case. Atomic units are used throughout the paper unless stated otherwise.

II. RADIATIVE RECOMBINATION

A. Original Kramers formula

In order to make our approach more transparent, we go first through the major points of derivation of the Kramers formula. We focus on the RR process, although a similar treatment works for the processes of one-photon and multiphoton ionization [49]. Consider field-free radiative electron capture by a Coulomb center with charge Z . Since most of the radiation occurs when the electron is close to the center, we will assume motion along a parabolic orbit with eccentricity ϵ close to 1. Then, using the classical theory of radiation [50], we obtain for the power radiated

$$I_s = \frac{64 \times 2^{2/3} s^{4/3} \mathcal{E}^4}{3c^3 Z^2} \left\{ (1 - \epsilon^2) \text{Ai}^2(u) + \left(\frac{2}{s} \right)^{2/3} (\text{Ai}')^2(u) \right\}, \quad (1)$$

where s is the harmonics order, $s = \omega T/2\pi$, ω is the frequency of the emitted radiation, T is the period of revolution of the electron on the orbit, \mathcal{E} is the electron energy on the orbit, and

$$u = \left(\frac{s}{2} \right)^{2/3} (1 - \epsilon^2).$$

Note that the Landau and Lifshitz [50] definition of the Airy function Φ differs by a constant factor from Ai:

$$\Phi(u) = \sqrt{\pi} \text{Ai}(u).$$

In the classical theory the harmonic order is a positive integer, and Eq. (1) is obtained from a more accurate expression for intensity of radiation of high harmonics for a motion on a bounded orbit, in terms of the Bessel function, assuming that the eccentricity of the orbit is close to 1, i.e., the orbit is close to a parabola. Accordingly,

$$1 - \epsilon \ll 1, \quad s \gg 1.$$

For a capture to a low-lying orbit these conditions might not be valid. However, the accurate expression cannot be used in the problem of RR because it assumes that the initial electron motion is already bound. The approximate Eq. (1) is more appropriate, since it describes the motion of the charged particle on the border between the unbounded and bounded motion. Moreover, the asymptotic expression for the Bessel function used in derivation of Eq. (1),

$$J_s(s\epsilon) \approx \left(\frac{2}{s} \right)^{1/3} \text{Ai} \left[\left(\frac{s}{2} \right)^{2/3} (1 - \epsilon^2) \right],$$

is valid for the noninteger s and works quite well for rather low values of s , down to 0.4. This explains the success of the

Kramers formula even for capture into the ground state, $n = 1$, when s is close to $1/2$. This is an important conclusion, which we will use for the laser-assisted recombination as well.

Using the correspondence principle, we obtain for the energy

$$\mathcal{E} = -\frac{Z^2}{2n^2},$$

for the period

$$T = \frac{2\pi n^3}{Z^2},$$

and for the eccentricity

$$1 - \epsilon^2 = \frac{l^2}{n^2},$$

where n is the principal quantum number, and l is the angular momentum quantum number.

Using these expressions, we can rewrite Eq. (1) as

$$I_s = \frac{4 \times 2^{4/3} \omega^{2/3} Z^{14/3}}{3c^3 n^6} [(Ai')^2(u) + uAi^2(u)].$$

The probability of emission of a photon for a given electron angular momentum l during the period is

$$P_l = \frac{T}{\omega} I_s = \frac{8\pi 2^{4/3} \omega^{2/3} Z^{8/3}}{3c^3 n^3 \omega} [(Ai')^2(u) + uAi^2(u)]. \quad (2)$$

We can relate l to the impact parameter b as

$$l = kb, \quad (3)$$

where k is the initial electron momentum. Then the total cross section for the radiative recombination is

$$\begin{aligned} \sigma &= 2\pi \int P(b) b db \\ &= \frac{64\pi^2 Z^4}{3c^3 n^3 4E_e \omega} \int_0^\infty [(Ai')^2(u) + uAi^2(u)] du, \end{aligned} \quad (4)$$

where we have expressed the electron momentum k in terms of the energy of the incident electron, $k = (2E_e)^{1/2}$, and used

$$u = \left(\frac{\omega}{2Z^2}\right)^{2/3} l^2$$

and Eq. (3), resulting in

$$bdb = \left(\frac{2Z^2}{\omega}\right)^{2/3} \frac{du}{2k^2}.$$

Although the maximum value of l is $n - 1$, we have extended the upper integration limit to infinity since the Airy function decays very fast with l . Physically this means that only the orbits with low l (or eccentricity close to 1) contribute to radiation. In this case the integral in Eq. (4) is easily evaluated using

$$[Ai'(u)Ai(u)]' = uAi^2(u) + (Ai')^2(u).$$

Therefore

$$\int_0^\infty [(Ai')^2(u) + uAi^2(u)] du = -Ai'(0)Ai(0) = \frac{1}{2\pi\sqrt{3}}.$$

Finally,

$$\sigma = \frac{8\pi Z^4}{3\sqrt{3}c^3 n^3 \omega_n E_e}, \quad (5)$$

where

$$\omega_n = E_e + \frac{Z^2}{2n^2}.$$

Equation (5) is the Kramers' result for the RR cross section. Note that it exhibits the correct threshold behavior: σ diverges as $1/E_e$ for low E_e .

B. Generalization to laser-assisted recombination

In the case of the presence of a laser field we use the electric dipole approximation and direct the incident electron velocity \mathbf{v}_0 parallel to the electric field. The force acting on the electron is chosen in the form

$$F = F_0 \cos(\omega t + \phi_0),$$

where F_0 is the amplitude and ϕ_0 is a constant phase. We direct both vectors along the x axis and start integration of classical trajectories with the following initial conditions: $x(0) = x_0$, $y(0) = b$, $v_x(0) = v_0$. We choose the initial position far enough from the Coulomb center so that the Coulomb interaction at $t = 0$ can be neglected. Accordingly, the initial dependence $v_x(t)$ is given by

$$v_x(t) = v_0 + \frac{F_0}{\omega} [\sin(\omega t + \phi_0) - \sin(\phi_0)]. \quad (6)$$

The results for the cross sections should be averaged over ϕ_0 . This is equivalent to averaging over the initial position x_0 [51].

For calculations we choose classical trajectories which start with an arbitrary large impact parameter b but eventually lead to orbits with low angular momentum l . At this point the electron is close to the Coulomb center, l becomes approximately constant, and the electron radiates according to the Kramers scenario. Typically the minimum value of the angular momentum l_{\min} correlates well with the small value of the distance of the closest approach r_{\min} . However, at initial energies close to zero this might be not the case; therefore we assign a nonzero value to the radiation probability only if r_{\min} is well within the zone where the Coulomb interaction dominates. After calculation of the radiation probability, the RR cross section is obtained as

$$\sigma^{RR} = 2\pi \int P[l_{\min}(b)] b db,$$

where P is the probability of radiation for a trajectory leading to the minimum (in absolute value) angular momentum l_{\min} , which is found by running trajectories in the superposition of the laser and Coulomb fields. The trajectories are computed by using the method described in Ref. [34]. After l_{\min} is found, the probability of RR to an orbit with the principal quantum number n is calculated using Eq. (2). The probability is non-negligible if

$$1 - \epsilon^2 = \frac{l^2}{n^2} \ll 1.$$

We will be interested in parameters of the laser for which the Coulomb focusing effect is important. First, from the studies of the laser-stimulated bremsstrahlung [34] we conclude that the mean electron velocity in the laser field, following

from Eq. (6),

$$\bar{v}_x = v_0 - \frac{F_0}{\omega} \sin \phi_0,$$

should be small to allow several oscillations before the electron hits the nucleus.

At this point it is convenient to introduce a parameter

$$\chi = \frac{\omega v_0}{F_0}.$$

For $\chi < 1$ there are two values of phase ϕ_0 , ϕ_1 and $\pi - \phi_1$, where

$$\phi_1 = \arcsin \chi,$$

corresponding to $\bar{v}_z = 0$. In the vicinity of these values the range of impact parameters contributing to the RR cross section becomes very large, in fact, as will be shown below, theoretically infinite. If $\chi > 1$ the cross section is finite, but it can still be large if χ is not greatly exceeding 1.

The electron quiver amplitude $a_0 = F_0/\omega^2$ should not be too large in order to allow for the Coulomb focusing to be efficient:

$$\frac{F_0}{\omega^2} = \frac{v_0}{\chi \omega} < a_1.$$

Choosing $a_1 = 100$ a.u., we get $\omega > 0.01 v_0$ a.u., $F_0 > 0.01 v_0^2$ a.u. For illustration we have chosen three examples: (1) $v_0 = 0.2$ a.u., $F_0 = 0.0056$ a.u. ($I = 1.10$ TW/cm²), $\omega = 0.014$ a.u. ($\lambda = 3.26$ μ m); (2) $v_0 = 0.1$ a.u., $F_0 = 0.000244$ ($I = 2.09$ GW/cm²), $\omega = 0.002$ ($\lambda = 22.8$ μ m); (3) $v_0 = 0.2$ a.u., $F_0 = 0.000244$, $\omega = 0.002$. The values of the parameter χ are 0.5000, 0.8197, and 1.639 in cases 1, 2, and 3, respectively. In all three cases we calculate the electron-proton recombination, that is, $Z = 1$.

As was discussed in the Introduction, for a realistic experiment the field should not be too strong, since an intense field can lead to a fast reionization of the captured electron. A possible restriction on the field intensity comes from the requirement that the RR rate be higher than the multiphoton ionization rate due to the laser field,

$$W^{RR} \gg W^{PI},$$

where

$$W^{RR} = \sigma^{RR} j$$

is the radiative recombination rate, W^{PI} is the photoionization rate, and j is the incident electron current density. A weaker restriction for excited states can be obtained from noticing that the excited state formed as a result of recombination is unstable with respect to spontaneous decay to a lower, typically ground state. If

$$W^{PI} < W^S,$$

where W^S is the rate of the spontaneous decay, then the excited state is not ionized but decays, and a stable atom is formed in the ground state.

At low frequencies corresponding to infrared and far-infrared radiation and moderate principal quantum numbers n ranging from 1 to 5, one-photon ionization is not possible. Thus in order to estimate the ionization rate we used the

TABLE I. Multiphoton ionization rates and spontaneous decay rates for the hydrogen atom. γ is the Keldysh parameter, and F_t is the threshold field for the classical over-the-barrier ionization. The spontaneous decay rate is given for $np \rightarrow 1s$ transitions, which have the highest probability for the $nl \rightarrow n'l'$ series. All quantities are listed in a.u.

	n	N_{\min}	γ	F_t	W^{PI}	W^S
Case 1	1	36	2.5	0.0625	5.0×10^{-38}	
	2	9	1.25	0.0039	2.13×10^{-3}	1.51×10^{-8}
Cases 2 and 3	2	63	4.10	0.0039	0	1.51×10^{-8}
	3	28	2.73	0.00077	1.30×10^{-23}	3.98×10^{-9}
	4	16	2.05	0.00024	2.38×10^{-6}	1.70×10^{-9}
	5	11	1.64	0.00010	19.52	0.82×10^{-9}

formula of Popruzhenko *et al.* [52], which works well for a wide range of values of the Keldysh parameter describing both tunneling and multiphoton regimes if $N_{\min} > n$, where N_{\min} is the minimum number of photons required to ionize the state with the principal quantum number n . (An alternative formula of Berson [49] works for small N_{\min} .) In Table I we present the values of ionization rates for hydrogen atoms and compare them with the spontaneous decay rates taken from Bethe and Salpeter [48] for the three cases chosen above. In case 1 (TW field) the rate appears too high even for $n = 2$, which is not surprising since the threshold field for the classical over-the-barrier ionization in this case is lower than the actual field, 0.0056 a.u. However, the ground state should survive against photoionization even for moderate electron currents. In cases 2 and 3 (GW field) states with $n = 1, 2$, and 3 should survive against photoionization both due to higher recombination rates and sufficiently short lifetimes with respect to spontaneous emission. However, for $n = 4$ the ionization rate is higher than the spontaneous decay rate.

III. RESULTS AND DISCUSSION

A. Radiation probabilities and cross sections

In Fig. 1 we present the minimum (in absolute value) angular momentum l_{\min} and the distance of the closest approach r_{\min} as functions of the impact parameter b for case 2, $\phi_0 = 0.51439$. Strictly speaking, l is the projection of the angular momentum on the axis perpendicular to the collision plane (the only nonzero component of the angular momentum); therefore it can be both positive and negative, and the quantity of interest is $|l|_{\min}$. Low values of $|l|_{\min}$, allowing efficient radiation, correlate very well with low values of r_{\min} , meaning that radiation occurs only at close approaches, which is physically reasonable. Typically a trajectory starts with high value of l , and it becomes low (if it does) only at small distances from the Coulomb center. Even for low b , when l_{\min} is naturally low, the distance of the closest approach is low as well.

In Figs. 2 and 3 we present the RR probability as a function of impact parameter. In cases 1 and 2 the parameter $\chi < 1$, and we choose phase ϕ_0 close to ϕ_1 . Note that $\phi_1 = \pi/6 = 0.52360$ in case 1 and $\phi_1 = 0.96084$ in case 2, meaning that in the first example ($\phi_0 = 0.51439$) the mean drift velocity in

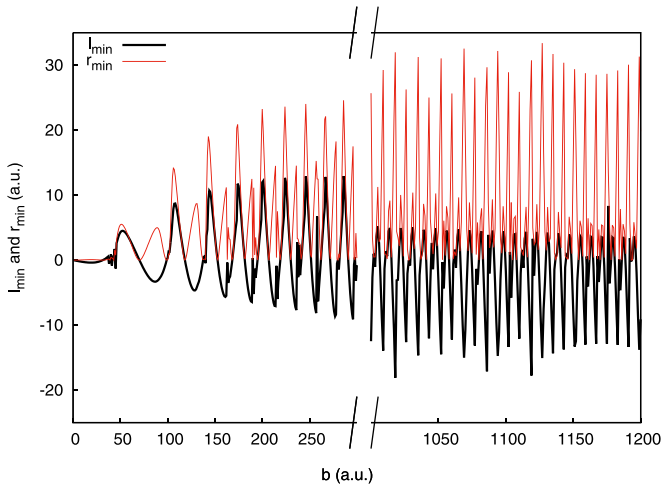


FIG. 1. Dependencies of the minimum angular momentum l_{\min} (thick black curve) and the distance of the closest approach (thin red curve) on the impact parameter b for $v = 0.1$ a.u., $F_0 = 0.000\ 244$ a.u., $\omega = 0.002$ a.u., $\phi_0 = 0.514\ 39$. Note that l_{\min} is the value of l corresponding to the minimum value of $|l|$.

the pure field \bar{v}_x is slightly positive and in the second example ($\phi_0 = 0.60$) slightly negative.

Two important features are apparent. First, the function $P(b)$ exhibits a fractal structure which is somewhat more regular in case 2. We demonstrate it in Fig. 2 by enlarged scales in panels (b) and (c). Second, in cases 1 and 2, when $\chi < 1$, $P(b)$ does not seem to decrease for high b . This can be understood in terms of Coulomb focusing: If the mean

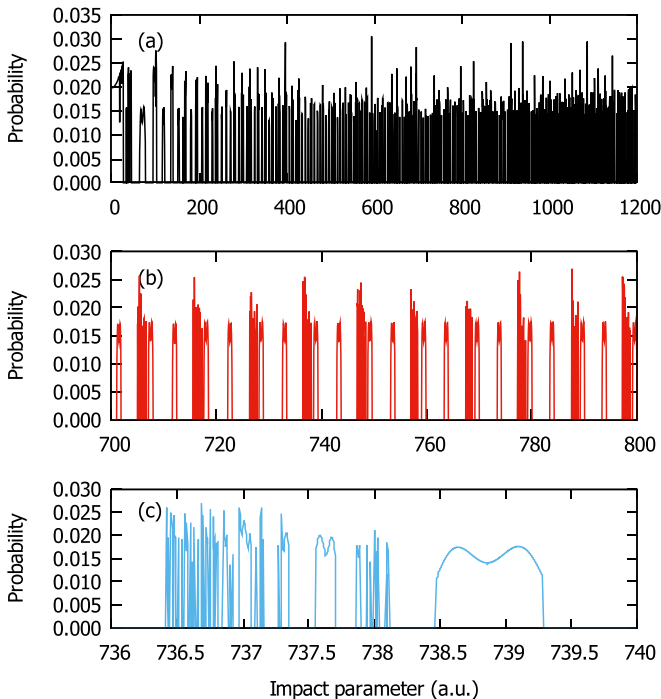


FIG. 2. RR probability for $n = 2$ as a function of the impact parameter b for $v = 0.2$ a.u., $F_0 = 0.0056$ a.u., $\omega = 0.0140$ a.u., and $\phi_0 = 0.514\ 39$. (b, c) Progressively enlarged scales in b .

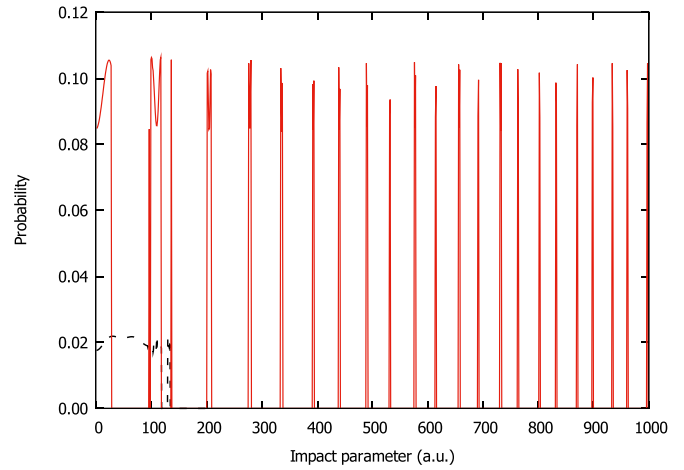


FIG. 3. RR probability for $n = 2$ as a function of the impact parameter for case 2 ($v = 0.1$ a.u., $F_0 = 0.000\ 244$ a.u., $\omega = 0.002$ a.u.), $\phi_0 = 0.92$ (solid red line), and case 3 ($v = 0.2$ a.u., $F_0 = 0.000\ 244$ a.u., $\omega = 0.002$ a.u.), $\phi_0 = 0.92$ (dashed black line).

drift velocity \bar{v}_x is small enough, the oscillating electron will be eventually brought close to the nucleus by the Coulomb force, even for large impact parameters. To demonstrate this, we present in Figs. 4 and 5 electron trajectories for case 1, $\phi_0 < \phi_1$ (Fig. 4), and $\phi_0 > \phi_1$ (Fig. 5). Even in the second example, when $\bar{v}_x < 0$, the Coulomb field is able to turn the trajectory around and to bring the electron to the Coulomb center. Panel (b) of Fig. 5 demonstrates the sensitivity of the radiation probability to the impact parameter. Although the values of the impact parameter are close for two trajectories ($b = 300$ and 304 a.u., respectively), only the first trajectory brings the electron close enough to the Coulomb center to lead to a substantial radiation probability. This effect is similar to that found in the bremsstrahlung problem [34] and explains the chaotic structure of the function $P(b)$. The radiation probability is less chaotic at low b , since the corresponding angular momentum in this case is low at the starting points of trajectories.

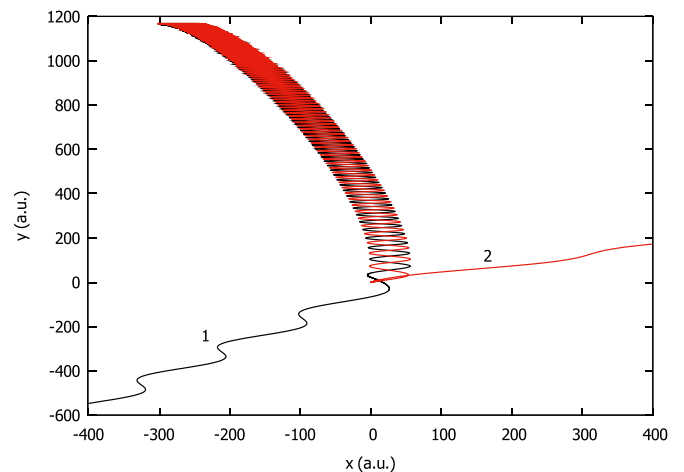


FIG. 4. Electron trajectories for case 1, $\phi_0 = 0.514\ 39$. Black line (curve 1): $b = 1166$ a.u.; red line (curve 2): $b = 1170$ a.u.

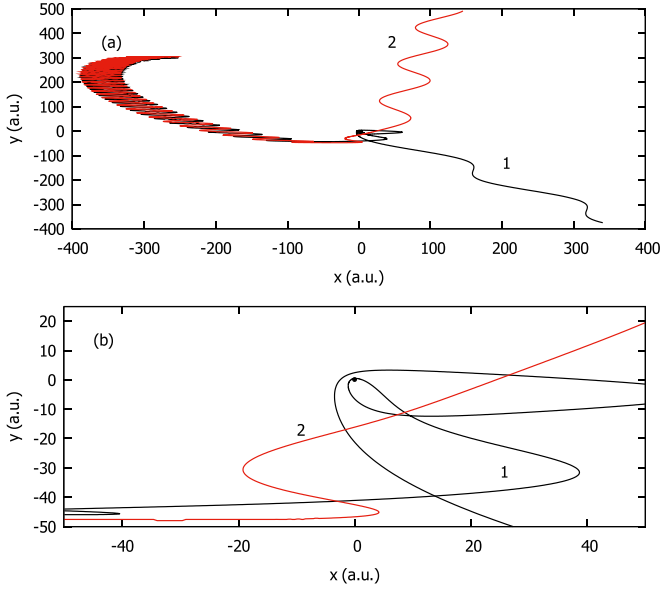


FIG. 5. Electron trajectories for case 1, $\phi_0 = 0.60$. Black line (curve 1): $b = 300$ a.u.; red line (curve 2): $b = 304$ a.u. Panel (b) shows the same trajectories on the enlarged scale near the Coulomb center which is marked by the full circle. The distance of the closest approach for the first trajectory is 0.47 a.u., which is not noticeable on the scale of drawing.

Further investigations show that $P(b)$ does not decrease at $b \rightarrow \infty$ in two narrow ranges of ϕ_0 close to ϕ_1 and $\pi - \phi_1$. In these ranges the radiative recombination cross section becomes theoretically infinite. However, in practice the range of impact parameters contributing to the total cross section is limited by several factors, including geometrical constraints (like a finite distance between electrons in the beam) and the finite laser pulse duration. For illustrative purposes we have limited the range of b by choosing a finite pulse duration t_p . In this case trajectories which require time t exceeding t_p to reach the Coulomb center do not contribute to the enhancement of the cross section. Since t depends on the initial electron position x_0 , in general the finite pulse duration leads to dependence of the RR cross section on x_0 (even after averaging over ϕ_0). However, if $\bar{v}_x t_p \gg |x_0|$, this dependence is negligible. Calculations show that for $t_p > 5$ ps and $|x_0|$ about a few hundred a.u., σ is independent of x_0 . For a continuous electron beam this would mean that the RR yield per one Coulomb center during the pulse duration is $\sigma j t_p$, and the gain in the yield (as compared to the field-free case) is exactly the same as the gain in the cross section σ .

In Fig. 6 we present the radiative recombination cross section as a function of ϕ_0 . To make the cross section finite in cases 1 and 2, we assumed $t_p = 5$ ps. The cross sections demonstrate two important features: first they exhibit the chaotic structure; second, for $\chi < 1$ (cases 1 and 2) they are large in the regions close to ϕ_1 and $\pi - \phi_1$.

Figure 7 compares the dependence of $\sigma(\phi_0)$ for two values of the laser pulse duration t_p . Although the peak value of the cross section grows faster than t_p , the averaged cross section grows somewhat slower than t_p . Somewhat unexpected is the double-peak structure in the vicinities of $\phi_0 = \phi_1$ and

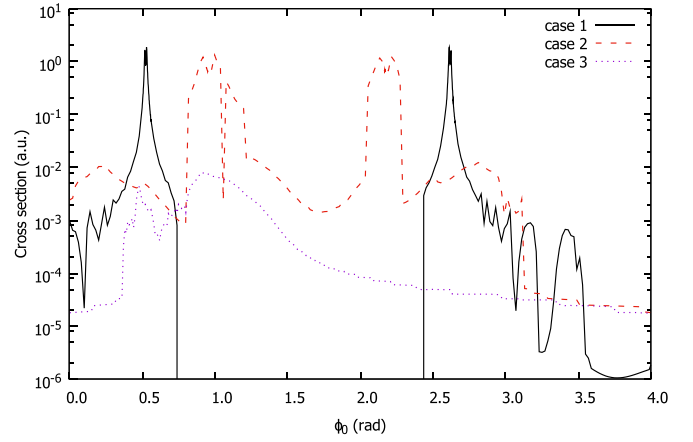


FIG. 6. Cross section for RR into the $n = 2$ state as a function of ϕ_0 . Solid black line: case 1; dashed red line: case 2; dotted purple line: case 3. The laser pulse duration in cases 1 and 2 is 5 ps.

$\phi_0 = \pi - \phi_1$. The local minima between the peaks are located exactly at these values of ϕ_0 , but the maxima correspond to slightly negative and slightly positive values of \bar{v}_x , of the order of 10^{-3} a.u.

In Table II we present the cross sections averaged over ϕ_0 and the gain factor due to the presence of the laser. Since in our calculations we use the same semiclassical approach as Kramers, we obtain the gain factor by dividing our cross section by that of Kramers. For $\chi < 1$ (cases 1 and 2) the gain factor is large and grows with the pulse duration t_p . But even in case 3, when $\chi > 1$, the gain factor is substantial. As was discussed in Sec. II, in the field $F_0 = 0.0056$ a.u. only the ground state survives against the multiphoton ionization; therefore the data for excited states in this case are more of academic rather than practical value. They might also be relevant to the HHG problem, where the survival of recombined atoms is of less importance.

In Fig. 8 we present the velocity dependence of the cross section for case 2. Note that by “velocity” we mean the

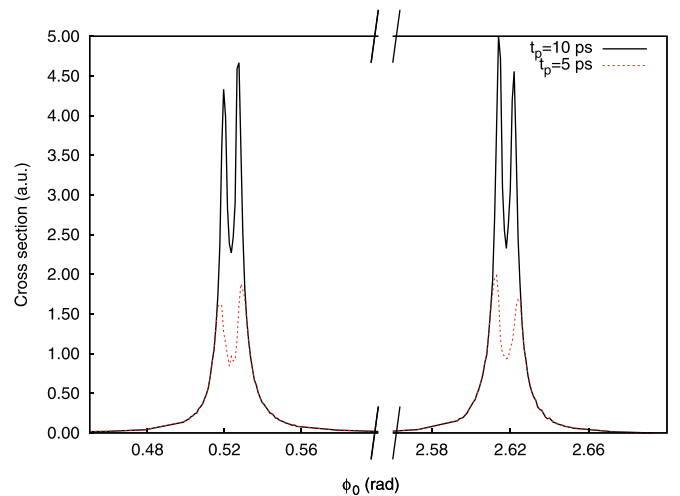


FIG. 7. Cross section for RR into the $n = 2$ state as a function of ϕ_0 for case 1, different laser pulse duration. Solid black line: $t_p = 10$ ps; dashed red line: $t_p = 5$ ps.

TABLE II. Radiative recombination cross sections and gain factors for the hydrogen atom. σ^{Kr} is the Kramers cross section. Cross sections are listed in a.u.

	n	σ	σ^{Kr}	Gain factor
Case 1, $t_p = 5$ ps	1	0.4102×10^{-1}	0.1807×10^{-3}	227.0
	2	0.1466×10^{-1}	0.8102×10^{-4}	180.9
	3	0.5478×10^{-2}	0.4607×10^{-4}	118.9
	4	0.2610×10^{-2}	0.2865×10^{-4}	91.1
Case 1, $t_p = 10$ ps	1	0.6387×10^{-1}	0.1807×10^{-3}	353.4
	2	0.2288×10^{-1}	0.8102×10^{-4}	282.5
	3	0.8558×10^{-2}	0.4607×10^{-4}	185.8
	4	0.4121×10^{-2}	0.2865×10^{-4}	143.8
Case 2 $t_p = 5$ ps	1	0.1652×10^0	0.7444×10^{-3}	221.9
	2	0.6523×10^{-1}	0.3615×10^{-3}	180.5
	3	0.3716×10^{-1}	0.2299×10^{-3}	161.6
	4	0.2512×10^{-1}	0.1620×10^{-3}	155.0
Case 3	1	0.1710×10^{-2}	0.1807×10^{-3}	9.462
	2	0.5681×10^{-3}	0.8102×10^{-4}	7.013
	3	0.3022×10^{-3}	0.4607×10^{-4}	6.560
	4	0.1960×10^{-3}	0.2865×10^{-4}	6.841

electron velocity v_0 outside the field region. After entering the field the mean electron energy outside the Coulomb zone is $v_0^2/2 + E_p$, where $E_p = F_0^2/4\omega^2$ is the ponderomotive energy. As a result, the laser-assisted cross section does not exhibit the $1/E_e$ singularity as the field-free cross section does. The laser-assisted cross section peaks at the value of v_0 close to F_0/ω corresponding to $\chi = 1$, and then drops sharply. Although the chaotic features in the dependence of cross section on ϕ_0 are essentially smoothed out after averaging over ϕ_0 , some small irregularities are still visible in the $\sigma(v_0)$ dependence.

Another substantial difference of the present case with the field-free case is that for a fixed initial electron energy the radiation spectrum does not consist of sharp lines corresponding to the photon energies $\omega_n = E_e + 1/(2n^2)$ but is broad due to a broad range of energy values E_c obtained by the electron when it approaches the Coulomb center. Due to the random (fractal) feature of the dependence $E_c(b)$, the photon spectrum also looks chaotic.

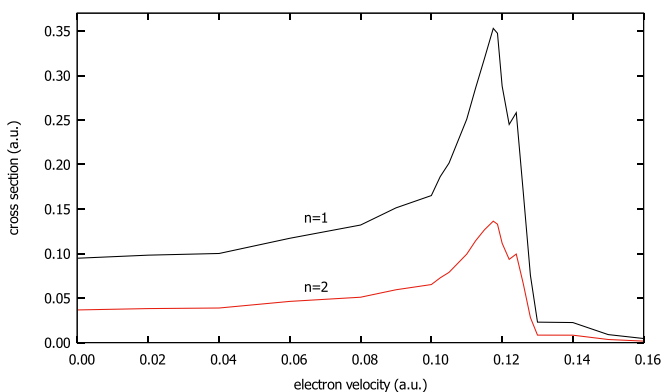


FIG. 8. Cross section for RR into the $n = 1$ and $n = 2$ states as a function of electron velocity for case 2, $t_p = 5$ ps.

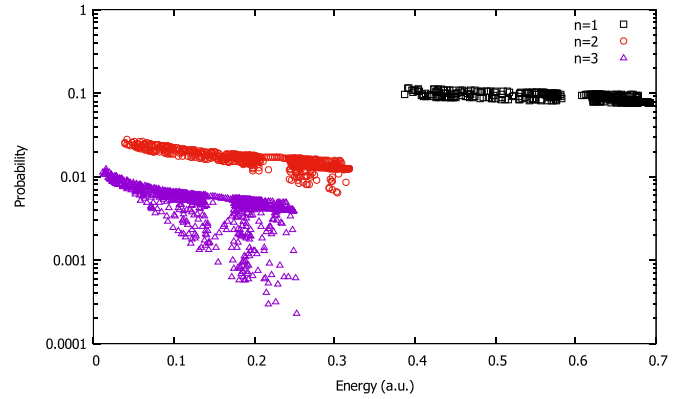


FIG. 9. Probability of emission of a photon with frequency as a function of energy of the emitted photon in case 1, $\phi_0 = \pi/6$.

In Fig. 9 we present the radiation spectrum for recombination to $n = 1, 2$, and 3 states for $\phi_0 = \pi/6$. Generally the spectrum is distributed chaotically within the range from about $\omega_n - 2E_p$ to $\omega_n + 4E_p$.

B. Chaos and quantum effects

Laser-assisted RR involves dynamical chaos, which is not usually discussed in quantum treatment of this and similar problems of electron-ion interaction in the presence of laser fields. RR is the final step in the HHG process which leads to a broad spectrum of the emitted photons, like in our case of laser-assisted RR. However, most quantum-mechanical calculations show that the harmonic spectrum in this case is regular. Moreover, it is usually interpreted in terms of just *two*, “short” and “long” electron trajectories [12] and does not require chaotic trajectories, some of which can lead to numerous revolutions of electrons about the Coulomb center. This can be explained by the different energy range involved: in the present paper we are concerned with low-energy electrons for which the Coulomb effect is essential. In contrast, in the HHG problem the interest is towards production of high-order harmonics, the process involving relatively high-energy electrons for which the Coulomb effects can be either neglected or treated perturbatively, like in the simple man model [11]. Note, however, that chaotic features in the photon spectrum were observed in quantum calculations [22,25] of RR.

The problem can be discussed from a much broader perspective. Quantum effects typically suppress chaos in corresponding classical systems [53,54]. A well-known example is the quantum suppression of classical chaotic diffusion in ionization of Rydberg atoms by microwaves [55,56]. Therefore it is natural to look for mechanisms of quantum suppression of chaos in the problem of electron motion in a superposition of the Coulomb and the laser fields. One of these mechanisms can be related to the quantum nature of the field [36]: in a quantum scattering process the electron cannot get or give off energy less than $\hbar\omega$. The other is related to the Coulomb singularity, which in a sense is suppressed in quantum mechanics due to the uncertainty principle. This might suggest that in classical simulations a soft Coulomb potential, widely used in problems of above-threshold ionization and HHG [57–59], rather than the singular Coulomb potential, should be used.

It was claimed [60], for example, that all observed features in microwave ionization can be explained by classical simulations with a soft Coulomb potential and do not require the quantum localization mechanism. However, some caution is required at this point. First, the soft Coulomb potential has been used a lot in quantum simulations with reasons which are completely different from those used in classical simulations. For example, in a model one-dimensional problem the Coulomb singularity becomes unphysical and should be removed. Even in two- and three-dimensional quantum simulations [22] the soft Coulomb potential was used just for computational convenience. Second, the preservation of the Coulomb singularity is often crucial for quantum-classical correspondence. For example, classical and quantum results for Rutherford scattering are identical, and this does not require Coulomb “softening.” A similar conclusion results from comparison of classical and quantum bremsstrahlung in the Coulomb field [34]. The last observation is particularly important for RR, since both RR and bremsstrahlung processes are dominated by close collisions when the Coulomb singularity is fully exposed.

We conclude that attempts to estimate quantum effects should not incorporate Coulomb “softening.” On the other hand, quantum effects might remove some chaotic features observed in the RR problem, for example, in the radiation probability as a function of phase ϕ_0 or in the radiation spectrum. Note, however, that some quantum calculations of RR [22] and HHG [61] exhibit spectra with chaotic features. In particular, van de Sand and Rost [61] connected these features with chaos in classical scattering.

IV. CONCLUSION

In conclusion, we have developed a semiclassical theory for laser-assisted radiative recombination using an approach similar to that of Kramers [47] for a field-free recombination. We expect that our results have the same accuracy as the Kramers formula. The obtained results demonstrate several important features. First they show how the spontaneous RR can be enhanced by using moderate-intensity infrared fields. This might have important applications to plasma processes [2] and antihydrogen formation [10]. Second, they exhibit interesting physics: the classical treatment of laser-assisted RR results in chaotic behavior of the radiation probability as a function of the impact parameter and the constant phase of the electric field. This happens because of the chaotic nature of the problem of Coulomb scattering in an external laser field investigated by Wiesenfeld [35–37]. What happens when quantum-mechanical effects are incorporated is not quite clear. Although some regularization of chaotic features is expected from a general theory, chaotic behavior of the radiation spectrum cannot be ruled out and in fact was observed in quantum-mechanical simulations [22,61]. Finally, due to the Coulomb focusing effect, the RR cross section for certain field parameters becomes very large—theoretically infinite. We make it finite by limiting the duration of the laser pulse and present sample results for t_p of 10 and 5 ps.

ACKNOWLEDGMENT

This work was supported by the US National Science Foundation under Grant No. PHY-1803744.

-
- [1] R. Flannery, *Atomic, Molecular, and Optical Physics Handbook* (AIP, Woodbury, NY, 1996).
 - [2] Y. Hahn, *Rep. Prog. Phys.* **60**, 691 (1997).
 - [3] G. I. Budker and A. N. Skrinsky, *Sov. Phys. Usp.* **21**, 277 (1978).
 - [4] M. Bell, J. Chaney, H. Herr, F. Krienen, P. Møller-Petersen, and G. Petrucci, *Nucl. Instrum. Methods* **190**, 237 (1981).
 - [5] R. Neumann, H. Poth, A. Winnacker, and A. Wolf, *Z. Physik* **313**, 253 (1983).
 - [6] U. Schramm, J. Berger, M. Grieser, D. Habs, E. Jaeschke, G. Kilgus, D. Schwalm, A. Wolf, R. Neumann, and R. Schuch, *Phys. Rev. Lett.* **67**, 22 (1991).
 - [7] F. B. Yousif, P. Van der Donk, Z. Kuchеровsky, J. Reis, E. Brannen, J. B. A. Mitchell, and T. J. Morgan, *Phys. Rev. Lett.* **67**, 26 (1991).
 - [8] M. L. Rogelstad, F. B. Yousif, T. J. Morgan, and J. B. A. Mitchell, *J. Phys. B* **30**, 3913 (1997).
 - [9] M. Amoretti, C. Amsler, G. Bonomi, P. D. Bowe, C. Canali, C. Carraro, C. L. Cesar, M. Charlton, A. M. Ejsing, A. Fontana, M. C. Fujiwara, R. Funakoshi, P. Geova, J. S. Hangst, R. S. Hayano, V. Jogensen, A. Kellerbauer, V. Lagomarsino, E. LodiRizzini, M. Macri *et al.* (ATHENA Collaboration) *Phys. Rev. Lett.* **97**, 213401 (2006).
 - [10] W. A. Bertsche, E. Butler, M. Charlton, and N. Madsen, *J. Phys. B* **48**, 232001 (2015).
 - [11] P. B. Corkum, *Phys. Rev. Lett.* **71**, 1994 (1993).
 - [12] P. Agostini and L. F. DiMauro, *Rep. Prog. Phys.* **67**, 813 (2004).
 - [13] P. B. Corkum and F. Krausz, *Nat. Phys.* **3**, 381 (2007).
 - [14] T. J. Bensity, M. B. Campbell, and R. R. Jones, *Phys. Rev. Lett.* **81**, 3112 (1998).
 - [15] E. S. Shuman, R. R. Jones, and T. F. Gallagher, *Phys. Rev. Lett.* **101**, 263001 (2008).
 - [16] V. Carrat, E. Magnuson, and T. F. Gallagher, *Phys. Rev. A* **92**, 063414 (2015).
 - [17] P. Krstic and Y. Hahn, *Phys. Rev. A* **50**, 4629 (1994).
 - [18] Y. Hahn and P. Krstic, *J. Phys. B* **27**, L509 (1994).
 - [19] A. Jaroń, J. Z. Kamiński, and F. Ehlötzky, *Phys. Rev. A* **61**, 023404 (2000).
 - [20] M. Y. Kuchiev and V. N. Ostrovsky, *Phys. Rev. A* **61**, 033414 (2000).
 - [21] D. B. Milošević and F. Ehlötzky, *Phys. Rev. A* **65**, 042504 (2002).
 - [22] S. X. Hu and L. A. Collins, *Phys. Rev. A* **70**, 013407 (2004).
 - [23] A. N. Zheltukhin, A. V. Flegel, M. V. Frolov, N. L. Manakov, and A. F. Starace, *J. Phys. B* **45**, 081001 (2012).
 - [24] R. A. Müller, D. Seipt, S. Fritzsche, and A. Surzhykov, *Phys. Rev. A* **92**, 053426 (2015).
 - [25] A. Čerkić and D. B. Milošević, *Phys. Rev. A* **88**, 023414 (2013).
 - [26] S. Odžak and D. B. Milošević, *Phys. Rev. A* **92**, 053416 (2015).
 - [27] A. Čerkić, M. Busuladžić, and D. B. Milošević, *Phys. Rev. A* **95**, 063401 (2017).
 - [28] K. C. Kulander, *Phys. Rev. A* **35**, 445(R) (1987).

- [29] D. Bauer and P. Koval, *Comput. Phys. Commun.* **174**, 396 (2006).
- [30] J. S. Parker, D. H. Glass, L. R. Moore, E. S. Smyth, K. T. Taylor, and P. G. Burke, *J. Phys. B* **33**, L239 (2000).
- [31] X.-M. Tong and S.-I. Chu, *Chem. Phys.* **217**, 119 (1997).
- [32] D. Peng, L.-W. Pi, M. V. Frolov, and A. F. Starace, *Phys. Rev. A* **95**, 033413 (2017).
- [33] L. D. Landau and E. M. Lifshitz, *Quantum Mechanics (Nonrelativistic Theory)* (Pergamon, Oxford, 1977).
- [34] H. B. Ambalampitiya and I. I. Fabrikant, *Phys. Rev. A* **99**, 063404 (2019).
- [35] L. Wiesenfeld, *Phys. Lett. A* **144**, 467 (1990).
- [36] L. Wiesenfeld, *Acta Phys. Pol., B* **23**, 271 (1992).
- [37] L. Wiesenfeld, *J. Phys. B* **25**, 4373 (1992).
- [38] B. Hu, J. Liu, and S.-G. Chen, *Phys. Lett. A* **236**, 533 (1997).
- [39] Th. Brabec, M. Yu. Ivanov, and P. B. Corkum, *Phys. Rev. A* **54**, R2551 (1996).
- [40] G. L. Yudin and M. Y. Ivanov, *Phys. Rev. A* **63**, 033404 (2001).
- [41] D. Comtois, D. Zeidler, H. Pépin, J. C. Kieffer, D. M. Villeneuve, and P. B. Corkum, *J. Phys. B* **38**, 1923 (2005).
- [42] D. Shafir, H. Soifer, C. Vozzi, A. S. Johnson, A. Hartung, Z. Dube, D. M. Villeneuve, P. B. Corkum, N. Dudovich, and A. Staudte, *Phys. Rev. Lett.* **111**, 023005 (2013).
- [43] S. A. Berman, C. Chandre, and T. Uzer, *Phys. Rev. A* **92**, 023422 (2015).
- [44] C. Huang, Q. Liao, Y. Zhou, and P. Lu, *Opt. Express* **18**, 14293 (2010).
- [45] J. Daněk, K. Z. Hatsagortsyan, and Ch. H. Keitel, *Phys. Rev. A* **97**, 063410 (2018).
- [46] J. Lu, Q. Li, L. He, and H. Qiao, *J. Phys. B* **52**, 035401 (2019).
- [47] H. A. Kramers, *Philos. Mag.* **46**, 836 (1923).
- [48] H. A. Bethe and E. Salpeter, *Quantum Mechanics of One and Two-Electron Atoms* (Springer, Berlin, 1957).
- [49] I. Berson, *Phys. Lett. A* **84A**, 364 (1981).
- [50] L. D. Landau and E. M. Lifshitz, *The Classical Theory of Fields: Course of Theoretical Physics*, 3rd ed. (Pergamon, Oxford, 1971), Vol. 2.
- [51] M. V. Fedorov and M. Yu. Ivanov, *Laser Phys.* **3**, 365 (1993).
- [52] S. V. Popruzhenko, V. D. Mur, V. S. Popov, and D. Bauer, *Phys. Rev. Lett.* **101**, 193003 (2008).
- [53] M. Berry, *Phys. Scr.* **40**, 335 (1989).
- [54] M. Berry, in *Chaos and Quantum Physics*, edited by M. J. Gianonni, A. Voros, and J. Zinn-Justin (Elsevier, Amsterdam, 1991), p. 251.
- [55] G. Casati, B. V. Chirikov, D. L. Shepelyansky, and I. Guarneri, *Phys. Rep.* **154**, 77 (1987).
- [56] G. Casati and L. Molinari, *Prog. Theor. Phys. Supp.* **98**, 287 (1989).
- [57] J. Javanainen, J. H. Eberly, and Q. Su, *Phys. Rev. A* **38**, 3430 (1988).
- [58] S. C. Rae, X. Chen, and K. Burnett, *Phys. Rev. A* **50**, 1946 (1994).
- [59] W. Becker, X. J. Liu, P. J. Ho, and J. H. Eberly, *Rev. Mod. Phys.* **84**, 1011 (2012).
- [60] M. Wójcik, J. Zakrzewski, and K. Rzążewski, *Phys. Rev. A* **52**, R2523 (1995).
- [61] G. van de Sand and J. M. Rost, *Phys. Rev. Lett.* **83**, 524 (1999).